Flavonoid-derived human phenyl-γ-valerolactone metabolites selectively detoxify amyloid-β oligomers and prevent memory impairment in a mouse model of Alzheimer's disease

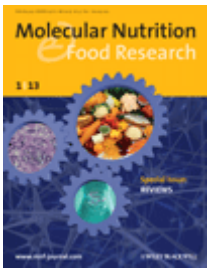

Flavonoid-derived human phenyl-γ-valerolactone metabolites selectively detoxify amyloid-β oligomers and prevent memory impairment in a mouse model of Alzheimer's disease

Journal:	*Molecular Nutrition and Food Research*
Manuscript ID	mnfr.201900890.R1
Wiley - Manuscript type:	Research Article
Date Submitted by the Author:	n/a
Complete List of Authors:	Ruotolo, Roberta; University of Parma, Department of Chemistry, Life Sciences and Environmental Sustainability Minato, Ilaria; University of Parma, Department of Chemistry, Life Sciences and Environmental Sustainability La Vitola, Pietro; Istituto di Ricerche Farmacologiche Mario Negri Sede di Milano, Department of Neuroscience Artioli, Luisa; Istituto di Ricerche Farmacologiche Mario Negri Sede di Milano, Department of Neuroscience Curti, Claudio; University of Parma, Department of Food & Drugs Franceschi, Valentina; University of Parma, Department of Medical-Veterinary Science Brindani, Nicoletta; University of Parma, Department of Food & Drugs Amidani, Davide; University of Parma, Department of Chemistry, Life Sciences and Environmental Sustainability Colombo, Laura; Istituto di Ricerche Farmacologiche Mario Negri Sede di Milano, Department of Molecular Biochemistry and Pharmacology Salmona, Mario; Istituto di Ricerche Farmacologiche Mario Negri Sede di Milano, Department of Molecular Biochemistry and Pharmacology Forloni, Gianluigi; Istituto di Ricerche Farmacologiche Mario Negri Sede di Milano, Department of Neuroscience Donofrio, Gaetano; University of Parma, Department of Medical-Veterinary Science Balducci, Claudia; Istituto di Ricerche Farmacologiche Mario Negri Sede di Milano, Department of Neuroscience Del Rio, Daniele; University of Parma, Department of Medical-Veterinary Science Ottonello, Simone; University of Parma, Dept. of Chemistry, Life Sciences and Environmental Sustainability
Keywords:	flavan 3-ol flavonoids, phenyl-γ-valerolactones, polyphenols, amyloid oligomer detoxification, Alzheimer's disease prevention

Flavonoid-derived human phenyl-γ-valerolactone metabolites selectively detoxify amyloid-β oligomers and prevent memory impairment in a mouse model of Alzheimer's disease

Roberta Ruotolo[1,#], Ilaria Minato[1,#], Pietro La Vitola[2], Luisa Artioli[2], Claudio Curti[3], Valentina Franceschi[4], Nicoletta Brindani[3,5], Davide Amidani[1,6], Laura Colombo[7], Mario Salmona[7], Gianluigi Forloni[2], Gaetano Donofrio[4], Claudia Balducci[2], Daniele Del Rio[4], Simone Ottonello[1,*]

[1]Department of Chemistry, Life Sciences and Environmental Sustainability, University of Parma, 43124 Parma, Italy

[2]Department of Neuroscience, IRCCS - Istituto di Ricerche Farmacologiche Mario Negri, 20156 Milan, Italy

[3]Department of Food & Drugs, University of Parma, 43124 Parma, Italy

[4]Department of Medical-Veterinary Science, University of Parma, 43126 Parma, Italy

[5]Present address: Istituto Italiano di Tecnologia (IIT) Central Research Labs, 16163 Genova, Italy

[6]Present address: Chiesi Farmaceutici S.p.A., R&D Department, 43122 Parma, Italy

[7]Department of Molecular Biochemistry and Pharmacology, IRCCS - Istituto di Ricerche Farmacologiche Mario Negri, 20156 Milan, Italy

[#]These authors contributed equally to this work

*Corresponding author:
Prof. Simone Ottonello
Department of Chemistry, Life Sciences and Environmental Sustainability
University of Parma
Parco area delle Scienze, 23/A
43124 Parma, ITALY
E-mail: simone.ottonello@unipr.it
Phone: +39 0521 905646 / FAX: +39 0521 905151

Abbreviations

AβO, amyloid-β oligomer; AD, Alzheimer's disease; AFM, atomic force microscopy; BBB, blood-brain barrier; CQ, clioquinol; EGCG, (−)-epigallocatechin gallate; 3-HBA, 3-hydroxybenzoic acid; 3-HPP, 3-hydroxyphenylpropionic acid; (4'-OH)-PVL, 5-(4'-hydroxyphenyl)-γ-valerolactone; ICV, intra-cerebroventricular; NORT, novel object recognition task; PEI, polyethylenimine; PHS, Public Health Service; PVL, phenyl-γ-valerolactone; SD, synthetic defined dextrose medium; TBS, Tris-buffered saline buffer.

Keywords

Flavan 3-ol flavonoids, phenyl-γ-valerolactones, polyphenols, amyloid oligomer detoxification, Alzheimer's disease prevention

Abstract

Scope

Amyloid-β oligomers (AβO) are causally related to Alzheimer's disease (AD). Dietary natural compounds, especially flavonoids and flavan-3-ols, hold great promise as potential AD-preventive agents but their host and gut microbiota metabolism complicates identification of the most relevant bioactive species. This study aims to investigate the ability of a comprehensive set of phenyl-γ-valerolactones (PVL), the main circulating metabolites of flavan-3-ols and related dietary compounds in humans, to prevent AβO-mediated toxicity.

Methods and results

The anti-AβO activity of PVLs was examined in different cell model systems using a highly toxic β-oligomer-forming polypeptide (β23) as target toxicant. Multiple PVLs, and particularly the monohydroxylated 5-(4'-hydroxyphenyl)-γ-valerolactone metabolite [(4'-OH)-PVL], relieved β-oligomer-induced cytotoxicity in yeast and mammalian cells. As revealed by atomic force microscopy (AFM) and other *in vitro* assays, (4'-OH)-PVL interferes with AβO (but not fibril) assembly and actively remodels preformed AβOs into non-toxic amorphous aggregates. In keeping with the latter mode of action, treatment of AβOs with (4'-OH)-PVL prior to brain injection strongly reduced memory deterioration as well as neuroinflammation in a mouse model of AβO-induced memory impairment.

Conclusion

PVLs, which have been validated as biomarkers of the dietary intake of flavan-3-ols, lend themselves as novel AβO-selective, candidate AD-preventing compounds.

1. Introduction

Age-related neurodegenerative diseases, which include sporadic Alzheimer's disease (AD) as one of the most prevalent, represent a major medical and societal challenge. Although the ultimate pathogenesis of many of these disorders is only partially known, most of them share the presence of amyloid aggregates, some of which, such as soluble prefibrillar amyloid-β oligomers (AβO) in the case of AD, are considered as the most proximal neurotoxic species.[1,2] AβOs are structurally and functionally polymorphic aggregates ranging in size from dimers up to multiple higher-order species that have been associated with various cytotoxic effects ultimately leading to neuroinflammation and cognitive impairment.[2,3] AβOs, which have been shown not to be obligate intermediates of the fibrillization pathway,[2,4] are nevertheless thought to be in a dynamic equilibrium with fibrillar aggregates and amyloid plaques, which are currently considered as potentially harmless Aβ storage forms.[1,5,6] According to this view, AβO accumulation resulting from drug-induced interference with plaque formation and/or promotion of their disaggregation has been proposed as a possible explanation for the failure of many candidate AD drugs that primarily target large Aβ aggregates rather than AβOs.[7,8] Another recently added complexity may stem from the unexpectedly high diversity of Aβ peptide variants found in the brain of AD patients, that may hamper recognition of many of their aggregate species by sequence-specific monoclonal antibodies.[9]

This largely unsatisfactory outlook has spurred great interest in various natural compounds, especially polyphenols, that in various experimental settings have proven capable of modifying different neuropathological features of AD and to promote Aβ peptide detoxification by either interfering with AβO formation and/or by inducing the conversion of pre-existing AβOs into non-toxic higher-order aggregates.[4,10-13] Special attention, in this context, has been given to flavan-3-ols, polycyclic flavonoids that are particularly abundant in cocoa, tea, berries, red wine and other plant-derived foods and beverages.[14-19] Much less investigated, instead, have been the human metabolites of flavan-3-ols, only a few of which have been shown to mitigate Aβ (including AβO) toxicity.[20]

Phenyl-γ-valerolactones (PVL) are the major group of circulating flavan-3-ol metabolites in humans.[18,21-24] As outlined in **Figure 1**, PVLs can originate from (−)-epicatechin but also from condensed epicatechins such as the dimeric procyanidin B2, through 5-carbon side-chain ring fission catalyzed by gut, mainly colonic, microbial enzymes and subsequent phase II metabolic conversion by host hepatic enzymes.[18,24] According to recent metabolic profiling studies in humans,[24] approximately 42% of ingested (−)-epicatechin is converted within 4 to 12 h into PVLs, which reached peak plasma levels within 6 h and were still well detectable after 24 h.[22] These data highlight the need to consider PVLs as potential AβO targeting compounds responsible for, or at least contributing to, the anti-neurodegenerative effects of dietary flavan-3-ols.[18]

To begin to address this issue in the context of AD-related amyloid proteopathy, we set out to evaluate the anti-AβO activity of a comprehensive set of PVLs (**Figure 1**). A newly developed *in vivo* yeast assay using as readout cell growth inhibition caused by a highly cytotoxic artificial polypeptide (β23) preferentially forming β-amyloid oligomeric species[25,26] was utilized for the initial screen. Multiple PVLs, including sulfated PVL derivatives but particularly the monohydroxylated metabolite 5-(4'-hydroxyphenyl)-γ-valerolactone [(4'-OH)-PVL], emerged as highly effective detoxifying compounds. A similar efficacy profile was observed in β23-overexpressing human cells and in other assays involving human $A\beta_{42}$-derived AβOs but not fibrils. Importantly, (4'-OH)-PVL also displayed a dose-dependent neuroprotective and anti-neuroinflammatory effect in an acute mouse model of AβO-induced memory impairment.

2. Experimental Section

2.1 Chemicals

PVL metabolites #1, #2 and #3 (see **Supporting Information Table S1**) were produced by asymmetric synthesis,[27] while compounds #4, #5, #6 and #7 were synthesized by functionalization of the corresponding aglycones.[28] PVLs were dissolved in DMSO as 20 mM stock solutions. Details for other compounds used in this manuscript can be found in **Supporting Information**.

2.2 Cytotoxicity assays in yeast

Yeast strains expressing different variants of the human $A\beta_{42}$ and β23 peptides were constructed as described in **Supporting Information Experimental Section** and **Table S2**.

For growth curve analysis, yeast transformants were cultured at 30°C for 24 h in 'non-inducing' synthetic defined dextrose (SD) medium containing 2% (w/v) glucose. Yeast pre-cultures were then washed, transferred to 96-well plates and diluted to an OD_{600} of 0.1 with 'inducing' selective minimal medium [2% galactose plus a non-repressing glucose concentration (0.005% w/v)]; cells diluted with SD medium served as controls. Cell growth was monitored for three days by OD_{600} measurements performed with a TriStar² LB 942 Microplate Reader (Berthold Technologies). Growth curves were determined in triplicate for each condition and analyzed with the GraphPad Prism software.

For serial dilution assays performed on solid media, yeast pre-cultures were washed, adjusted to an OD_{600} value of 1.0 and serially diluted in ten-fold increments, prior to spotting (4 µl aliquots for each dilution) onto glucose- or galactose-containing, selective minimal medium agar plates. Yeast growth was examined by visual inspection after incubation at 30°C for two days.

For compound screening, pre-cultures of the two-copy β23 integrative transformant were diluted to an OD_{600} of 0.1 with 'inducing' selective minimal medium. Aliquots of cells (198 µl each) were then dispensed into 96-well plates and 2 µl of each compound (from a 100X stock solution in DMSO) or DMSO only (vehicle) were added and assayed in triplicate upon incubation at 30°C for 48 h without agitation, followed by OD_{600} determination. The anti-β23 toxicity effect exerted by individual compounds is expressed as percentage of cell viability relative to the vehicle control (arbitrarily set to 0%). EC_{50} values, i.e., compound concentrations causing a 50% maximal protective effect, were extrapolated from dose-response curves (determined in triplicate for each compound) using GraphPad Prism.

2.3 Immuno-dot blot analysis

Yeast cell extracts for immuno-dot blot were prepared as described in **Supporting Information**.

Immuno-dot blot analysis was performed in a 96-well plate format using a Bio-Dot® microfiltration apparatus (Bio-Rad) for vacuum-transfer of the samples to nitrocellulose membranes (0.2 µm pore-size; Bio-Rad) pre-wetted with Tris-buffered saline (TBS; 20 mM Tris-HCl pH 7.5, 0.8% NaCl). Sample-loaded membranes were then blocked by incubation for 2 hours at room temperature in TTBS buffer (TBS supplemented with 0.1% Tween 20) containing 5% (w/v) BSA and 1% (w/v) fish skin gelatin. After blocking, replica stripes of the same membranes were incubated overnight at 4°C with the anti-amyloid oligomer antibody A11 (Thermo Fisher Scientific; 1:1000 dilution) and with an anti-Pgk1 antibody (Abcam; 1:2000 dilution) as loading control. Following washing with TTBS, membranes were incubated for 2 h at room temperature with IRDye-labeled goat anti-rabbit (for A11) or goat anti-mouse (for anti-Pgk1) secondary antibodies (LI-COR Biosciences; 1:15000 dilution), washed once more with TTBS, dried, and visualized with an Odyssey® fluorescence infrared imaging system (LI-COR Biosciences).

For immuno-dot blot analysis of the preformed AβOs (see below), an anti-β-amyloid, 1-16 antibody (6E10, BioLegend; 1:2000 dilution) was used as reference primary antibody, followed by incubation with the IRDye-labeled goat anti-mouse secondary antibody.

2.4 Proteotoxicity assays in mammalian cells

Molecular cloning procedures of the pC1 plasmids expressing the EGFP-$A\beta_{42}$ fusion protein, the E22G 'arctic' variant of $A\beta_{42}$ and the β23 polypeptide were detailed in **Supporting Information**. After sequence verification, the above plasmids were transfected into human embryo kidney 293T (HEK293) cells. HEK293 cells were cultured in DMEM medium (Thermo Fisher Scientific) containing 10% fetal bovine serum, 2 mM L-glutamine (Gibco), 50 IU/mL penicillin (Gibco), 50 µg/mL streptomycin (Sigma-Aldrich) and 2.5 µg/mL amphotericin B (Gibco) and were incubated at 37°C/5% CO_2 in a humidified incubator. Confluent cells in 48-well plates were transiently transfected with the pC1 plasmids, using a polyethylenimine (PEI)-based transfection reagent (Polysciences, Inc.) as per manufacturer's instructions.

Cell viability was measured 72 h after transfection with the MTT assay as described previously.[29] Three biological replicates (each comprising eight technical replicates/compound plus controls)

were performed for each compound. EC_{50} values (i.e., compound concentrations causing 50% maximum protection) were determined as described above for yeast proteotoxicity assays.

2.5 In vitro $A\beta_{42}$ oligomer and fibril formation

A depsipeptide derivative of the human $A\beta_{42}$ peptide (#RP10017 from GenScript; or in-house synthesized[30]) was used to prepare seed-free solutions of monomeric $A\beta_{42}$ as described previously.[31,32] Following $A\beta_{42}$ release by addition of 3 mM NaOH, the resulting $A\beta_{42}$ peptide solution was diluted with PBS to a final concentration of 100 µM and immediately used for AβO or fibril formation. AβOs for pre- and post-assembly assays and for intra-cerebroventricular (ICV) brain injection, were produced by incubating the above $A\beta_{42}$ monomer solution for 24 hours at 4°C. To test for the effect of (4'-OH)-PVL on AβO formation, (4'-OH)-PVL or the vehicle were added to the above $A\beta_{42}$ solution immediately after dilution with PBS. For post-assembly assays, AβOs preformed as described above were diluted 10-fold with PBS, supplemented with either (4'-OH)-PVL or the vehicle, and incubated at 22°C for three hours prior to atomic force microscopy (AFM) analysis. A similar experimental set-up was employed for immuno-dot blot analysis (see above) of the effect of (4'-OH)-PVL on preformed AβOs using 6E10 and A11 as reference and test primary antibodies. For fibril formation, the $A\beta_{42}$ monomer solution was incubated for 4 days at 37°C under acidic conditions (pH 5.0) in the presence of (4'-OH)-PVL or the vehicle. Before ICV brain injection, all AβO preparations were checked by AFM and size exclusion chromatography as described previously.[31,32]

2.6 Atomic force microscopy

Multimode AFM analysis was performed with a NanoScope V microscope (Bruker) operated in tapping mode using 0.01–0.025 Ohm–cm Antimony doped Si probes (thickness range, 3.75 µm; length, 125 µm; width, 35 µm; spring constant, 40 N/m) and a scan rate proportional to the scanned area (0.5–0.9 Hz), as described previously.[32] Twenty microliters of AβOs or fibrils were added to freshly cleaved mica at room temperature, after 10 min the samples were washed with MilliQ water and dried under a gentle stream of nitrogen. AFM images were analyzed for diameter

and length with the Scanning Probe Image Processor (SPIP data analysis package 5.1.6 v.). Topographic patterns and SPIP characterization were confirmed by independent measurements performed on a minimum of 4 different, spatially separated areas.

2.7 Behavioural and glial-histochemical analyses on AβO-injected mice

For ICV brain microinfusion of AβOs, a 7-mm long, stainless steel guide cannula was implanted by a stereotaxic surgery apparatus (model 900, David Kopf Instruments) into the cerebral lateral ventricle (L ± 1.0; DV-3.0 from dura) of forane (IsoFlo®, Zoetis)-anesthetized eight-weeks-old C57BL6/N male mice (see **Supporting Information** for details on animal care conditions). The familiarization phase of the novel object recognition task (NORT) was started 2 h after AβO injection and was followed 24 h later by the 'test phase' as described previously.[31] Memory performance was expressed as discrimination index, i.e., (seconds spent on novel object – seconds spent on familiar object)/(total time spent on both objects). At the end of the experiments, mice were sacrificed and the correct placement of the cannula into the lateral ventricle was verified histologically.

For neuro-histochemical analyses, brain slices from AβO-injected mice were incubated with 1% H_2O_2 for 10 min followed by a 1 h incubation at 4°C in blocking solution and an overnight incubation with anti-GFAP (Merck Millipore; 1:3500 dilution) and anti-Iba1 (FUJIFILM Wako Pure Chemical Corporation; 1:500 dilution) primary antibodies, as described previously[33] (see **Supporting Information** for further details).

2.8 Quantification and statistical analysis

Statistical significance of the differences measured in cell-based toxicity assays conducted on the different test compounds, NORT and histological data were evaluated by a one-way between-subjects ANOVA; Student's t-test was used for comparisons of only two groups, whereas the Tukey's posthoc test was used for multiple comparisons. The number of animals (n) utilized for each experiment/condition was specified in the corresponding figure legends. No specific method was employed for mice randomization being mice simply C57BL/6 naïve of very similar ages (7/8

weeks). Statistical analysis was performed with the GraphPad Prism v6.0. For all analyses significance was defined as $*$ $p < 0.05$, $**$ $p < 0.01$, $***$ $p < 0.001$.

3. Results

3.1 A highly sensitive yeast model system to assess β-amyloid oligomer-induced cytotoxicity

The yeast *Saccharomyces cerevisiae*, which is known to recapitulate a number of basic cellular features of amyloid-induced cytotoxicity,[34] was chosen as the initial model system in which to assess the anti-AβO activity of PVLs. Yeast cells proved to be quite tolerant to the human $A\beta_{42}$ peptide when expressed as a free cytosolic peptide (including its hypertoxic 'arctic' variant) or fused to scaffold proteins such as thioredoxin or EGFP[35-37] (**Supporting Information Fig. 1**). A more stringent but still relatively weak phenotype could be obtained by targeting $A\beta_{42}$ to the secretory pathway (HDEL-$A\beta_{42}$)[38] (**Supporting Information Fig. 1**).

To obtain a more sensitive cellular β-amyloid toxicity readout, we resorted to β23, a highly toxic artificial β-sheet polypeptide with a marked propensity to form soluble prefibrillar oligomeric aggregates both *in vitro*[26] and *in vivo*.[25] Indeed, when expressed from a multicopy vector under the control of a galactose-inducible promoter, β23 caused a readily detectable but exceedingly strong cell-death phenotype (**Fig. 2A**). We thus switched to a stably integrated form of β23 and inserted one copy and two copies of a galactose-inducible β23-encoding gene into the genome of an efflux-deficient (*pdr1Δpdr3Δ*) yeast strain. These integrative transformants displayed copy number-dependent cell growth inhibition phenotypes of different severity under both solid and liquid medium culture conditions (**Fig. 2A-B**). Because of the severe but still manageable growth inhibition caused by stable integration of two copies of β23, which may afford optimal sensitivity in the detection of phenotype modifying compounds, this integrative transformant was selected for the subsequent screening of PVLs. Importantly, as revealed by an immuno-dot blot analysis performed with an antibody (A11) that selectively recognizes toxic AβOs,[12,39] induction of β23 expression upon switch to a galactose-containing medium was accompanied by the accumulation of A11-immunoreactive, amyloid oligomeric material (**Fig. 2C**).

3.2 PVLs relieve β23-induced cytotoxicity in yeast

The above described β23 integrative transformant was employed for the screening of the whole set of polyphenol-related compounds (**Supporting Information Table S1**) using cell viability as readout. The metal-chelator clioquinol (CQ), for which different anti-Aβ and AD protective effects have previously been documented in various experimental settings,[40-43] including yeast cells expressing HDEL-$A\beta_{42}$,[44] was also included as an additional reference compound. As shown in **Figure 3A** and in **Supporting Information Table S3**, all PVL metabolites prevented β23-induced growth inhibition to some extent. However, the magnitude and dose-dependency of this effect varied significantly for the different PVLs. Preservation of cell viability ranged from approximately 14% for the 3',4'-dihydroxylated and the 3',4'-disulfated PVLs (#2 and #7 in **Fig. 1**) to up to 41% for the 3'-sulfated PVL metabolite (#5). Intermediate values were obtained with the other PVLs, the most effective of which was the monohydroxylated (4'-OH)-PVL metabolite (#1), which improved cell viability by 35% compared to the vehicle and also featured the lowest half-maximal effective concentration (EC_{50} = 498 pM; **Supporting Information Table S3**).

The β23 yeast assay was also applied to non-PVL polyphenol compounds previously shown to interfere with Aβ aggregation and to mitigate β-amyloid toxicity in various model systems.[11,20,45,46] These included (−)-epigallocatechin gallate (EGCG), a plant metabolite that can reach the systemic circulation, albeit at extremely low levels,[47] and has previously been shown to be considerably more active than the parent compounds,[48-50] and the human flavan-3-ol metabolites 3-hydroxybenzoic acid (3-HBA) and 3-hydroxyphenylpropionic acid (3-HPP). These compounds also scored positive in the yeast β23 assay but with lower activities and apparently higher (10- to 20-fold) EC_{50} values compared to (4'-OH)-PVL (**Supporting Information Table S3** and **Fig. S2**). Similar results (23% rescue of cell viability with an EC_{50} of 254 nM; **Supporting Information Table S3**) were obtained with the metal chelator CQ. Altogether, these results validate the β23-based yeast assay as a reliable tool for detecting compounds capable of relieving AβO-induced cytotoxicity and point to PVLs as highly protective compounds.

Based on the above observations and on the sub-nanomolar EC_{50} value displayed by (4'-OH)-PVL, we selected this particular monohydroxylated flavan-3-ol metabolite as lead for subsequent analyses and asked whether (4'-OH)-PVL treatment interferes with the accumulation of A11-reactive, β23 oligomeric species. As shown in **Figure 3B**, (4'-OH)-PVL and other PVLs (#5 and #6) markedly reduced A11 immunoreactivity in β23-expressing cells. While not excluding the possible occurrence of indirect, viability-promoting effects, this result suggests a direct mode of action, involving either β23 aggregation inhibition or oligomer detoxification.

3.3 Anti-β23 activity of PVLs in human cells

We next wished to find out whether the anti-β23 oligomer activity of PVLs observed in yeast also applies to human cells. To this end, we transferred the β23 coding sequence, as well as sequences coding for human $A\beta_{42}$ fused to EGFP[25] and its aggregation-prone 'arctic' variant, into a mammalian cell expression vector. This was followed by transfection and viability testing in HEK293 cells -the same cells employed for the initial characterization of the molecular bases of β23 cytotoxicity.[25]

Also in human cells, β23 proved to be significantly more toxic than the $A\beta_{42}$ peptide[25] and caused an approximately 50% lethality 72 h after transfection (**Supporting Information Fig. S3A**). We then examined the anti-proteotoxicity (and cell survival-promoting) activity of the different PVL metabolites. As shown in **Supporting Information Fig. S3B**, also in HEK293 cells, PVLs positively affected the viability of β23 expressing cells. (4'-OH)-PVL, which preserved cell viability by 96% compared to the vehicle control, was the second most effective compound, again with a very low half-maximal effective concentration (EC_{50} = 0.1 pM; **Supporting Information Table S4**). The main deviation from the yeast data was observed for the 5-(3',4'-dihydroxyphenyl)-γ-valerolactone metabolite (#2 in **Fig. 1**), which was the worst performing in the yeast β23 assay, whereas it afforded full viability in HEK293 cells although with an EC_{50} several orders of magnitude higher than that of (4'-OH)-PVL.

We then compared (4'-OH)-PVL activity with that of a subset of the anti-$A\beta_{42}$ reference compounds previously shown to relieve β23 cytotoxicity in the yeast system. As shown in **Supporting**

Information Table S4 and **Figure S3C**, also in human cells (4'-OH)-PVL was more active than CQ and the flavan-3-ol metabolites 3-HPP and 3-HBA, with a higher maximal protective capacity and a considerably lower (2-3 orders of magnitude) EC_{50} value.

3.4 (4'-OH)-PVL activity on human $A\beta_{42}$

We then examined the activity of (4'-OH)-PVL on the human $A\beta_{42}$ peptide. We first investigated the ability of (4'-OH)-PVL to relieve cytotoxicity caused by HDEL-$A\beta_{42}$, a fusion derivative of $A\beta_{42}$ that is forced into the secretory pathway.[38] As shown in **Supporting Information Figure S4**, also in this assay, (4'-OH)-PVL dose-dependently ameliorated the viability of yeast cells expressing HDEL-$A\beta_{42}$.

To further investigate the apparently oligomer-specific action of (4'-OH)-PVL, we examined the ability of (4'-OH)-PVL to interfere with $A\beta_{42}$ aggregation using AFM. Two distinct incubation conditions of the synthetic $A\beta_{42}$ peptide, carried out in the presence of (4'-OH)-PVL or vehicle, were utilized for these experiments: a 24 h incubation at 4°C (pH 7.4) for Aβ oligomers (**Fig. 4A**) and a longer (4 days) incubation at 37°C under acidic conditions for fibril formation (**Fig. 4B**). As shown in **Figure 4A**, (4'-OH)-PVL, at a 3:1 molar ratio with respect to monomeric $A\beta_{42}$, significantly reduced both AβO abundance and size compared to the vehicle alone. In contrast, it only slightly interfered with $A\beta_{42}$ fibril formation (**Fig. 4B**) and no significant effect of (4'-OH)-PVL could be detected in an *in vitro* $A\beta_{42}$ fibrillization assays conducted in the presence of thioflavin T (data not shown).

Given prior reports on the ability of polyphenol aglycones of different size and chemical structure to remodel soluble AβOs into large-size, unstructured and non-toxic aggregates,[11,12,51] we next examined the remodeling activity of (4'-OH)-PVL. To this end, preformed AβOs were treated with either vehicle or (4'-OH)-PVL and were imaged by AFM. As shown in **Figure 4C**, remodeling of AβOs into large-size amorphous aggregates was observed upon treatment with (4'-OH)-PVL (3:1 molar ratio with respect to monomeric $A\beta_{42}$) but not vehicle. Under the same experimental conditions, treatment with (4'-OH)-PVL caused a strong reduction of immunoreactivity with the β-oligomer-specific antibody A11 (**Fig. 4D**).

3.5 (4'-OH)-PVL prevents memory impairment and attenuates neuroinflammation in an acute mouse model of AβO-induced neurotoxicity

Following-up to the AβO detoxification activity revealed by *in vitro* experiments (**Fig. 4**), we investigated the effect of (4'-OH)-PVL in an acute mouse model of AβO-induced memory impairment.[31] Memory impairment measured with NORT in mice intra-cerebroventricularly injected with preformed AβOs was used as readout to evaluate a possible neuroprotective effect of (4'-OH)-PVL. To this end, C57BL/6 naïve mice were ICV microinjected with untreated AβOs or AβOs preincubated for 15 min with (4'-OH)-PVL at monomeric $A\beta_{42}$:PVL molar concentration ratios ranging from 1:1 to 1:10. As shown in **Figure 5**, AβOs caused a statistically significant memory impairment that was dose-dependently relieved by (4'-OH)-PVL. At the highest concentration (10 μM), (4'-OH)-PVL preserved 'novel object recognition' capacity by up to 84% of the vehicle control value, without any significant detrimental effect on the NORT performance when injected alone. Given the relationship between AβOs, glia and astrocyte activation,[52] neuroinflammation and AD,[53] we finally asked whether the above processes could also be modulated by (4'-OH)-PVL. To this end, mice were separately microinjected with vehicle, (4'-OH)-PVL (3 μM), preformed AβOs (1 μM) alone or preincubated for 15 min with (4'-OH)-PVL at a submaximal concentration (3 μM) that was already quite effective in preventing AβO-induced memory deterioration (**Fig. 5**). After 4 h, mice were sacrificed and hippocampal brain sections from animals belonging to the different treatment and control groups were immunostained with antibodies directed against the microglia/macrophage-specific protein Iba1 and the glia/astrocyte intermediate filament protein GFAP. The post-treatment 4 h time-point was chosen for neuroinflammation assessment because a significant AβO-mediated glial activation was previously observed at this particular time-point.[52] As shown in **Figure 6**, Iba1 and GFAP immunoreactivity significantly increased in AβO-injected mice and both biomarkers were reduced in brain sections from mice injected with (4'-OH)-PVL-preincubated AβOs compared with untreated AβOs. The reduction in Iba1 immunoreactivity proved to be statistically significant (*p*-value=0,0236; **Fig. 6A**), whereas a detectable but statistically non-significant trend toward a reduced immunoreactivity (*p*-value=0,1057) was observed in the case of

the astrocyte activation biomarker GFAP (**Fig. 6B**). The anti-AβO and memory preservation effect of (4'-OH)-PVL may thus also rely on a positive modulation of AβO-induced neuroinflammation.

4. Discussion

Based on a cross-species exploration focused on β-amyloid oligomer-induced cytotoxicity, this work documents the anti-AβO action of the PVL metabolites of flavan-3-ols, the major class of flavonoids in the human diet.[18,24]

The oligomer-focused configuration of the β23 assay developed and validated in this work may explain the marked target specificity of PVLs compared to other, more promiscuous (i.e., both amyloid oligomer- and fibril-active) compounds.[4] Since prefibrillar oligomeric aggregates and fibers are being increasingly viewed as opposite ends of the Aβ peptide toxicity range,[1,2,6] a selective, yet sequence-independent,[9] action on AβOs is currently considered a highly desirable feature of Aβ toxicity modifiers.[2]

We found that multiple PVLs alleviate β23 toxicity in yeast and HEK293 cells at sub-nanomolar concentrations, with an efficacy generally higher than that of previously known natural or synthetic anti-Aβ compounds. The monohydroxylated metabolite (4'-OH)-PVL proved to be particularly effective, and it relieved neurotoxicity caused by micromolar concentrations of intra-brain injected AβO at nearly stoichiometric concentrations, with a concomitant attenuation of both memory impairment and neuroinflammation.[31] As revealed by AFM analysis (**Fig. 5**), (4'-OH)-PVL interfered with AβO formation and converted preformed AβOs into large-size non-toxic aggregates with no evidence of oligomer disassembly. This AβO remodeling effect, which was previously shown to coincide with AβO detoxification,[11,12,51] may be central to the memory preservation and anti-neuroinflammatory action of PVLs.

Based on the AβO remodeling activity of chemically diverse polyphenol compounds, and the lack of such activity for the phenolic monomer resorcinol, a structure-activity relationship hypothesis has been proposed.[12] According to this hypothesis, the presence of two phenolic rings would appear to be minimally required for AβO remodeling. This seems at variance with the observed remodeling activity of the small-sized (4'-OH)-PVL metabolite, which contains only one monohydroxylated

phenolic ring but fused to the γ-valerolactone moiety via a one-carbon bridge. Interestingly, the relative efficacy of the different PVLs observed in cell-based assays suggests that while the presence of two hydroxyl groups (as in metabolite #2) does not appear to confer a superior anti-proteotoxic activity, the presence of at least one hydroxyl group (preferably at position 4', as in metabolites #1 and #5) seems to correlate with a stronger efficacy (**Figure 3**; **Supporting Information Figure S3B**, **Tables S3** and **S4**). Still, the significant residual activity displayed by hydroxyl-lacking PVLs such as #4 and #7 points to a potentially important contribution of the γ-valerolactone unit.

Additional biological activities of PVLs, some of which may be relevant to their ability to relieve AβO-induced memory impairment and neuroinflammation, have been reported previously.[18] These include pro-neuritogenic,[54] anti-inflammatory[55] and antioxidant activities.[56] The existence of a positive correlation between intake of flavan-3-ol rich foods (especially cocoa[15,16]) and cognitive performance has also been documented.[17,19] Notably, an enhancement of dentate gyrus function and cognition, attributed to an improved brain microcirculation, has been reported in healthy 50-69 year-old subjects who consumed a high cocoa flavan-3-ol containing diet.[57]

An important issue not addressed in the present study regards the ability of the tested PVLs to cross the blood-brain barrier (BBB). We note, however, that different PVLs scored positive in artificial BBB model systems, where 5-(3',4'-dihydroxyphenyl)-γ-valerolactone (#2)[54] and 5-(4'hydroxyphenyl)-γ-valerolactone-3'-sulfate (#5)[58] displayed high penetration capacities. Although brain PVL levels are difficult to predict, the bioavailability and prevalence of PVLs as long-lasting flavan-3-ol metabolites (elimination half-life ~6 h) along with their sub-micromolar peak plasma concentrations (>500 nM)[22,24] suggest that potentially effective, cumulative brain PVL levels might be reached, at least in response to a flavan-3-ol rich diet. Also relevant, in this regard, is the validation of PVLs as urine biomarkers of the intake (and prospective anti-neurodegenerative effects) of flavan-3-ols in ongoing epidemiological studies.[18,23,24] Given the key role of microbial enzymes in the initial ring fission reaction that gives rise to PVLs and increasing evidence suggesting that gut microbes can affect brain pathophysiology,[59] future studies will also need to

address the relationship between the gut microbiota composition and PVL production as well as the potential nutraceutical use of synthetic PVLs as AD-preventive compounds.

Acknowledgments

We thank the laboratory of the late Dr. Susan Lindquist (Whitehead Institute for Biomedical Research, Department of Biology, MIT and Howard Hughes Medical Institute, Cambridge, Massachusetts, USA) for the *pdr1Δpdr3Δ* mutant strain and Dr. Olivier Dangles (INRA, Avignon, France) for the kind gift of urolithin A, urolithin B and urolithin B-glucuronide. We also thank Johnny Habchi and Sean Chia from the laboratory of Dr. Michele Vendruscolo (Centre for Misfolding Diseases, Department of Chemistry, University of Cambridge, Cambridge, UK) for their kind help with *in vitro* $A\beta_{42}$ fibrillization assays. The contribution of Martina Sperindé and Elena Longhin to the setting-up of the yeast β23 screening system as part of their master thesis work, access to the central instrumentation facilities of CIM (University of Parma) and technical support by the Interuniversity Consortium for Biotechnology (CIB) are also gratefully acknowledged. This work was supported by grants from the University of Parma (FIL Program) to S.O. and MIUR (FFABBR 2017) to R.R.

Author Contributions

RR: yeast assays, data-analysis, drafting and critical revision of the manuscript. IM: yeast assays, data-analysis, preparation of $A\beta_{42}$ material for AFM and immune dot-blot analysis. PLV: AβO-mediated memory impairment experiments. LA: brain immunostaining experiments. CC: setting-up and supervision of the chemical synthesis and NMR verification of PVL metabolites. VF: amyloid toxicity assays in human cells. NB: chemical synthesis of PVL metabolites. DA and LC: AFM experiments. MS: supervision of AFM analysis. GF: supervision and critical assessment of neuroinflammation experiments. GD: design and supervision of human cells experiments. CB: design and supervision of NORT experiments, data analysis and critical revision of the manuscript. DDR: selection of candidate polyphenol metabolites and basic study design. SO: study concept,

data analysis and interpretation, manuscript writing, interaction with partner laboratories and funding retrieval.

Declaration of interests

The authors declare no competing interests.

5. References

[1] C. Haass, D. J. Selkoe, *Nat. Rev. Mol. Cell Biol.* **2007**, *8*, 101.

[2] E. N. Cline, M. A. Bicca, K. L. Viola, W. L. Klein, *J. Alzheimers Dis.* **2018**, *64*, S567.

[3] G. Forloni, C. Balducci, *J. Alzheimers Dis.* **2018**, *62*, 1261.

[4] M. Necula, R. Kayed, S. Milton, C. G. Glabe, *J. Biol. Chem.* **2007**, *282*, 10311.

[5] T. Tomiyama, T. Nagata, H. Shimada, R. Teraoka, A. Fukushima, H. Kanemitsu, H. Takuma, R. Kuwano, M. Imagawa, S. Ataka, Y. Wada, E. Yoshioka, T. Nishizaki, Y. Watanabe, H. Mori, *Ann. Neurol.* **2008**, *63*, 377.

[6] Z. X. Wang, L. Tan, J. Liu, J. T. Yu, *Mol. Neurobiol.* **2016**, *53*, 1905.

[7] F. Panza, M. Lozupone, G. Logroscino, B. P. Imbimbo, *Nat. Rev. Neurol.* **2019**, *15*, 73.

[8] H. Hara, F. Ono, S. Nakamura, S. E. Matsumoto, H. Jin, N. Hattori, T. Tabira, *J. Alzheimers Dis.* **2016**, *54*, 1047.

[9] J. Hodgson, *Nature biotechnology* **2019**, *37*, 114.

[10] D. E. Ehrnhoefer, J. Bieschke, A. Boeddrich, M. Herbst, L. Masino, R. Lurz, S. Engemann, A. Pastore, E. E. Wanker, *Nat. Struct. Mol. Biol.* **2008**, *15*, 558.

[11] J. Bieschke, J. Russ, R. P. Friedrich, D. E. Ehrnhoefer, H. Wobst, K. Neugebauer, E. E. Wanker, *Proc. Natl. Acad. Sci. U. S. A.* **2010**, *107*, 7710.

[12] A. R. Ladiwala, M. Mora-Pale, J. C. Lin, S. S. Bale, Z. S. Fishman, J. S. Dordick, P. M. Tessier, *Chembiochem : a European journal of chemical biology* **2011**, *12*, 1749.

[13] J. Wang, M. G. Ferruzzi, L. Ho, J. Blount, E. M. Janle, B. Gong, Y. Pan, G. A. Gowda, D. Raftery, I. Arrieta-Cruz, V. Sharma, B. Cooper, J. Lobo, J. E. Simon, C. Zhang, A. Cheng, X. Qian, K. Ono, D. B. Teplow, C. Pavlides, R. A. Dixon, G. M. Pasinetti, *J. Neurosci.* **2012**, *32*, 5144.

[14] A. Nehlig, *Br. J. Clin. Pharmacol.* **2013**, *75*, 716.

[15] L. Dubner, J. Wang, L. Ho, L. Ward, G. M. Pasinetti, *J. Alzheimers Dis.* **2015**, *48*, 879.

[16] A. Moreira, M. J. Diogenes, A. de Mendonca, N. Lunet, H. Barros, *J. Alzheimers Dis.* **2016**, *53*, 85.

[17] V. Socci, D. Tempesta, G. Desideri, L. De Gennaro, M. Ferrara, *Front. Nutr.* **2017**, *4*, 19.

[18] P. Mena, L. Bresciani, N. Brindani, I. A. Ludwig, G. Pereira-Caro, D. Angelino, R. Llorach, L. Calani, F. Brighenti, M. N. Clifford, C. I. R. Gill, A. Crozier, C. Curti, D. Del Rio, *Nat. Prod. Rep.* **2019**, *36*, 714.

[19] B. N. Jaeger, S. L. Parylak, F. H. Gage, *Mol. Aspects Med.* **2018**, *61*, 50.

[20] D. Wang, L. Ho, J. Faith, K. Ono, E. M. Janle, P. J. Lachcik, B. R. Cooper, A. H. Jannasch, B. R. D'Arcy, B. A. Williams, M. G. Ferruzzi, S. Levine, W. Zhao, L. Dubner, G. M. Pasinetti, *Mol. Nutr. Food Res.* **2015**, *59*, 1025.

[21] D. Del Rio, L. Calani, C. Cordero, S. Salvatore, N. Pellegrini, F. Brighenti, *Nutrition* **2010**, *26*, 1110.

[22] J. I. Ottaviani, G. Borges, T. Y. Momma, J. P. Spencer, C. L. Keen, A. Crozier, H. Schroeter, *Sci. Rep.* **2016**, *6*, 29034.

[23] J. I. Ottaviani, R. Fong, J. Kimball, J. L. Ensunsa, A. Britten, D. Lucarelli, R. Luben, P. B. Grace, D. H. Mawson, A. Tym, A. Wierzbicki, K. T. Khaw, H. Schroeter, G. G. C. Kuhnle, *Sci. Rep.* **2018**, *8*, 9859.

[24] G. Borges, J. I. Ottaviani, J. J. J. van der Hooft, H. Schroeter, A. Crozier, *Mol. Aspects Med.* **2018**, *61*, 18.

[25] H. Olzscha, S. M. Schermann, A. C. Woerner, S. Pinkert, M. H. Hecht, G. G. Tartaglia, M. Vendruscolo, M. Hayer-Hartl, F. U. Hartl, R. M. Vabulas, *Cell* **2011**, *144*, 67.

[26] M. W. West, W. Wang, J. Patterson, J. D. Mancias, J. R. Beasley, M. H. Hecht, *Proc. Natl. Acad. Sci. U. S. A.* **1999**, *96*, 11211.

[27] C. Curti, N. Brindani, L. Battistini, A. Sartori, G. Pelosi, P. Mena, F. Brighenti, F. Zanardi, D. Del Rio, *Adv. Synth. Catal.* **2015**, *357*, 4082.

[28] N. Brindani, P. Mena, L. Calani, I. Benzie, S. W. Choi, F. Brighenti, F. Zanardi, C. Curti, D. Del Rio, *Mol. Nutr. Food Res.* **2017**, *61*.

[29] G. Donofrio, S. Herath, C. Sartori, S. Cavirani, C. F. Flammini, I. M. Sheldon, *Reproduction* **2007**, *134*, 183.

[30] M. Beeg, M. Stravalaci, A. Bastone, M. Salmona, M. Gobbi, *Anal. Biochem.* **2011**, *411*, 297.

[31] C. Balducci, M. Beeg, M. Stravalaci, A. Bastone, A. Sclip, E. Biasini, L. Tapella, L. Colombo, C. Manzoni, T. Borsello, R. Chiesa, M. Gobbi, M. Salmona, G. Forloni, *Proc. Natl. Acad. Sci. U. S. A.* **2010**, *107*, 2295.

[32] M. Messa, L. Colombo, E. del Favero, L. Cantu, T. Stoilova, A. Cagnotto, A. Rossi, M. Morbin, G. Di Fede, F. Tagliavini, M. Salmona, *J. Biol. Chem.* **2014**, *289*, 24143.

[33] C. Balducci, G. Santamaria, P. La Vitola, E. Brandi, F. Grandi, A. R. Viscomi, M. Beeg, M. Gobbi, M. Salmona, S. Ottonello, G. Forloni, *Neurobiol. Aging* **2018**, *70*, 128.

[34] V. Khurana, S. Lindquist, *Nat. Rev. Neurosci.* **2010**, *11*, 436.

[35] T. von der Haar, L. Josse, P. Wright, J. Zenthon, M. F. Tuite, *Neurodegener. Dis.* **2007**, *4*, 136.

[36] F. D'Angelo, H. Vignaud, J. Di Martino, B. Salin, A. Devin, C. Cullin, C. Marchal, *Dis. Model. Mech.* **2013**, *6*, 206.

[37] A. Villar-Pique, S. Ventura, *Biochim. Biophys. Acta* **2013**, *1833*, 2714.

[38] S. Treusch, S. Hamamichi, J. L. Goodman, K. E. Matlack, C. Y. Chung, V. Baru, J. M. Shulman, A. Parrado, B. J. Bevis, J. S. Valastyan, H. Han, M. Lindhagen-Persson, E. M. Reiman, D. A. Evans, D. A. Bennett, A. Olofsson, P. L. DeJager, R. E. Tanzi, K. A. Caldwell, G. A. Caldwell, S. Lindquist, *Science* **2011**, *334*, 1241.

[39] R. Kayed, E. Head, J. L. Thompson, T. M. McIntire, S. C. Milton, C. W. Cotman, C. G. Glabe, *Science* **2003**, *300*, 486.

[40] P. A. Adlard, R. A. Cherny, D. I. Finkelstein, E. Gautier, E. Robb, M. Cortes, I. Volitakis, X. Liu, J. P. Smith, K. Perez, K. Laughton, Q. X. Li, S. A. Charman, J. A. Nicolazzo, S. Wilkins, K. Deleva, T. Lynch, G. Kok, C. W. Ritchie, R. E. Tanzi, R. Cappai, C. L. Masters, K. J. Barnham, A. I. Bush, *Neuron* **2008**, *59*, 43.

[41] H. LeVine, 3rd, Q. Ding, J. A. Walker, R. S. Voss, C. E. Augelli-Szafran, *Neurosci. Lett.* **2009**, *465*, 99.

[42] C. Grossi, S. Francese, A. Casini, M. C. Rosi, I. Luccarini, A. Fiorentini, C. Gabbiani, L. Messori, G. Moneti, F. Casamenti, *J. Alzheimers Dis.* **2009**, *17*, 423.

[43] T. M. Ryan, B. R. Roberts, G. McColl, D. J. Hare, P. A. Doble, Q. X. Li, M. Lind, A. M. Roberts, H. D. Mertens, N. Kirby, C. L. Pham, M. G. Hinds, P. A. Adlard, K. J. Barnham, C. C. Curtain, C. L. Masters, *J. Neurosci.* **2015**, *35*, 2871.

[44] K. E. Matlack, D. F. Tardiff, P. Narayan, S. Hamamichi, K. A. Caldwell, G. A. Caldwell, S. Lindquist, *Proc. Natl. Acad. Sci. U. S. A.* **2014**, *111*, 4013.

[45] Y. T. Choi, C. H. Jung, S. R. Lee, J. H. Bae, W. K. Baek, M. H. Suh, J. Park, C. W. Park, S. I. Suh, *Life Sci.* **2001**, *70*, 603.

[46] X. Y. Qin, Y. Cheng, L. C. Yu, *Neurosci. Lett.* **2012**, *513*, 170.

[47] M. Pervin, K. Unno, A. Takagaki, M. Isemura, Y. Nakamura, *Int. J. Mol. Sci.* **2019**, *20*.

[48] K. Rezai-Zadeh, D. Shytle, N. Sun, T. Mori, H. Hou, D. Jeanniton, J. Ehrhart, K. Townsend, J. Zeng, D. Morgan, J. Hardy, T. Town, J. Tan, *J. Neurosci.* **2005**, *25*, 8807.

[49] S. Bastianetto, Z. X. Yao, V. Papadopoulos, R. Quirion, *Eur. J. Neurosci.* **2006**, *23*, 55.

[50] Z. Najarzadeh, H. Mohammad-Beigi, J. Nedergaard Pedersen, G. Christiansen, T. V. Sonderby, S. A. Shojaosadati, D. Morshedi, K. Stromgaard, G. Meisl, D. Sutherland, J. Skov Pedersen, D. E. Otzen, *Biomolecules* **2019**, *9*.

[51] A. R. Ladiwala, J. C. Lin, S. S. Bale, A. M. Marcelino-Cruz, M. Bhattacharya, J. S. Dordick, P. M. Tessier, *J. Biol. Chem.* **2010**, *285*, 24228.

[52] C. Balducci, A. Frasca, M. Zotti, P. La Vitola, E. Mhillaj, E. Grigoli, M. Iacobellis, F. Grandi, M. Messa, L. Colombo, M. Molteni, L. Trabace, C. Rossetti, M. Salmona, G. Forloni, *Brain Behav. Immun.* **2017**, *60*, 188.

[53] M. T. Heneka, M. J. Carson, J. El Khoury, G. E. Landreth, F. Brosseron, D. L. Feinstein, A. H. Jacobs, T. Wyss-Coray, J. Vitorica, R. M. Ransohoff, K. Herrup, S. A. Frautschy, B. Finsen, G. C. Brown, A. Verkhratsky, K. Yamanaka, J. Koistinaho, E. Latz, A. Halle, G. C. Petzold, T. Town, D. Morgan, M. L. Shinohara, V. H. Perry, C. Holmes, N. G. Bazan, D. J. Brooks, S. Hunot, B. Joseph, N. Deigendesch, O. Garaschuk, E. Boddeke, C. A. Dinarello, J. C. Breitner, G. M. Cole, D. T. Golenbock, M. P. Kummer, *Lancet Neurol.* **2015**, *14*, 388.

[54] K. Unno, M. Pervin, A. Nakagawa, K. Iguchi, A. Hara, A. Takagaki, F. Nanjo, A. Minami, Y. Nakamura, *Mol. Nutr. Food Res.* **2017**, *61*.

[55] C. C. Lee, J. H. Kim, J. S. Kim, Y. S. Oh, S. M. Han, J. H. Y. Park, K. W. Lee, C. Y. Lee, *Int. J. Mol. Sci.* **2017**, *18*.

[56] A. Takagaki, S. Otani, F. Nanjo, *Biosci. Biotechnol. Biochem.* **2011**, *75*, 582.

[57] A. M. Brickman, U. A. Khan, F. A. Provenzano, L. K. Yeung, W. Suzuki, H. Schroeter, M. Wall, R. P. Sloan, S. A. Small, *Nat. Neurosci.* **2014**, *17*, 1798.

[58] D. Angelino, D. Carregosa, C. Domenech-Coca, M. Savi, I. Figueira, N. Brindani, S. Jang, S. Lakshman, A. Molokin, J. F. Urban, Jr., C. D. Davis, M. A. Brito, K. S. Kim, F. Brighenti, C. Curti, C. Blade, J. M. Del Bas, D. Stilli, G. I. Solano-Aguilar, C. N. D. Santos, D. Del Rio, P. Mena, *Nutrients* **2019**, *11*.

[59] G. M. Pasinetti, R. Singh, S. Westfall, F. Herman, J. Faith, L. Ho, *J. Alzheimers Dis.* **2018**, *63*, 409.

Figure Legends

Figure 1. Outline of human flavan-3-ol metabolism and PVL formation. Starting from (–)-epicatechin and procyanidin B2, chosen as representative plant polyphenol precursors, after 5-carbon side-chain ring fission and initial transformation catalyzed by gut microbial enzymes, compounds #1-2 serve as precursors for subsequent phase II metabolism as indicated. The latter is catalyzed by host colonic and hepatic enzymes and generates the indicated sulfated PVL derivatives (compounds #4-7) as major products (collectively designated as 'phase II metabolites') that are then released into the circulation.

Figure 2. β23 amyloid oligomer formation and toxicity in yeast. A) Serial dilution assays (10-fold input cell dilutions ranging from 10^1 to 10^4) were performed on yeast cells transformed with either episomal (*2μ*) or integrative β23 [one-copy (*1X*); two-copy (*2X*)] constructs; empty-vector (*ev*) transformants served as controls. Cells were spotted on glucose- or galactose-containing agar plates and growth was assessed after 2 days at 30°C. **B**) Growth curves of the 1X and the 2X β23 integrative transformants cultured under β23 expression repressive (+ glucose; *left*) or inducing (+ galactose; *right*) conditions. **C**) Immuno-dot blot analysis performed with the anti-amyloid oligomer antibody A11 on whole cell extract samples derived from the 2X β23 integrative transformant strain cultured in SD (glucose-containing) or SGal (galactose-containing) liquid medium. Immunoreactivity with the constitutively expressed phoshoglycerate kinase (*Pgk1*) enzyme served as a loading control.

Figure 3. PVLs protect against β23 toxicity and reduce the accumulation of A11-reactive amyloid oligomers in yeast cells. A) Dose-response plots of the protective effects of the different PVLs. The results are expressed as percentage of 2X β23 cell viability relative to the vehicle (VEH; arbitrarily set to 0%); data are the mean ± SD of three replicates. A schematic representation of the chemical structures of the tested PVLs is shown above individual bar-plots. **B**) Immuno-dot blot analysis performed with the A11 antibody on total lysates from 2X β23 cells cultured under inducing (+ galactose) conditions in the presence of the indicated PVLs or the vehicle. *Pdr1Δpdr3Δ*

cells treated with the vehicle served as reference; Pgk1 immunoreactivity was used as a loading control.

Figure 4. (4'-OH)-PVL interferes with $A\beta_{42}$ oligomer but not fibril formation and remodels preformed AβOs. A) AβOs were produced by incubating the synthetic human $A\beta_{42}$ depsipeptide for 24 h at 4°C (pH 7.4) in the presence of (4'-OH)-PVL (1:3 $A\beta_{42}$:PVL molar ratio), or the vehicle (VEH). A histogram quantification of the number ('*frequency*') and size ('*volume*') of the AβOs formed in the presence or absence of (4'-OH)-PVL is shown in the *right-side panel*. **B**) Same experimental set-up as in (A), but with a 4-days incubation at 37°C (pH 5.0) to allow for fibril formation. For each sample, height and amplitude AFM images are shown. **C**) Preformed AβOs produced as in (A) were diluted 10-fold with PBS supplemented with either (4'-OH)-PVL (1:3 monomeric $A\beta_{42}$:PVL molar ratio) or vehicle and incubated at 22°C for 3 h prior to AFM analysis. **D**) Immuno-dot blot analysis of preformed AβOs treated with (4'-OH)-PVL or the vehicle as in (C). The Aβ sequence-specific (6E10) and the oligomer conformation-specific (A11) antibodies were used as loading control and test antibodies, respectively. The monomeric (freshly dissolved) $A\beta_{42}$ peptide served as a negative control for A11-immunoreactivity.

Figure 5. (4'-OH)-PVL antagonizes AβO-mediated memory impairment. Histogram representation (mean ± SEM) of the Discrimination Index (see 'Experimental Section') measured by NORT in mice ICV-injected with AβOs (1 μM monomeric $A\beta_{42}$) preincubated with the vehicle (VEH; n=18) or the indicated concentrations of (4'-OH)-PVL [1 μM (n=7); 3 μM (n=21); 10 μM (n=10)]. Two additional groups of animals, ICV-injected in parallel with the vehicle (n=21) or with the highest concentration of (4'-OH)-PVL (10 μM; n=8) without AβOs served as controls. The significant memory deficit observed in the AβOs+VEH group compared to the VEH only group was dose-dependently antagonized by (4'-OH)-PVL (* $p<0.05$, *** $p<0.001$; Tukey's test).

Figure 6. (4'-OH)-PVL treatment reduces glial activation in AβO-treated mice. A) Hippocampal slices from mice microinjected with the vehicle (VEH, n=8), (4'-OH)-PVL (3 μM; n=8), preformed AβOs (1 μM monomeric $A\beta_{42}$) preincubated with VEH (n= 9), or with (4'-OH)-PVL (3 μM; n=9), were immuno-stained with an antibody against the microglia/macrophage-specific protein Iba1.

Immunoreactivity data (mean ± SEM) are reported in the histogram shown below the immuno-microscopy images (* p<0.05, *** p<0.001; Tukey's test). **B**) Same as (A) except for the use of an antibody directed against the glia/astrocyte intermediate filament protein GFAP for immunostaining (** p<0.01).

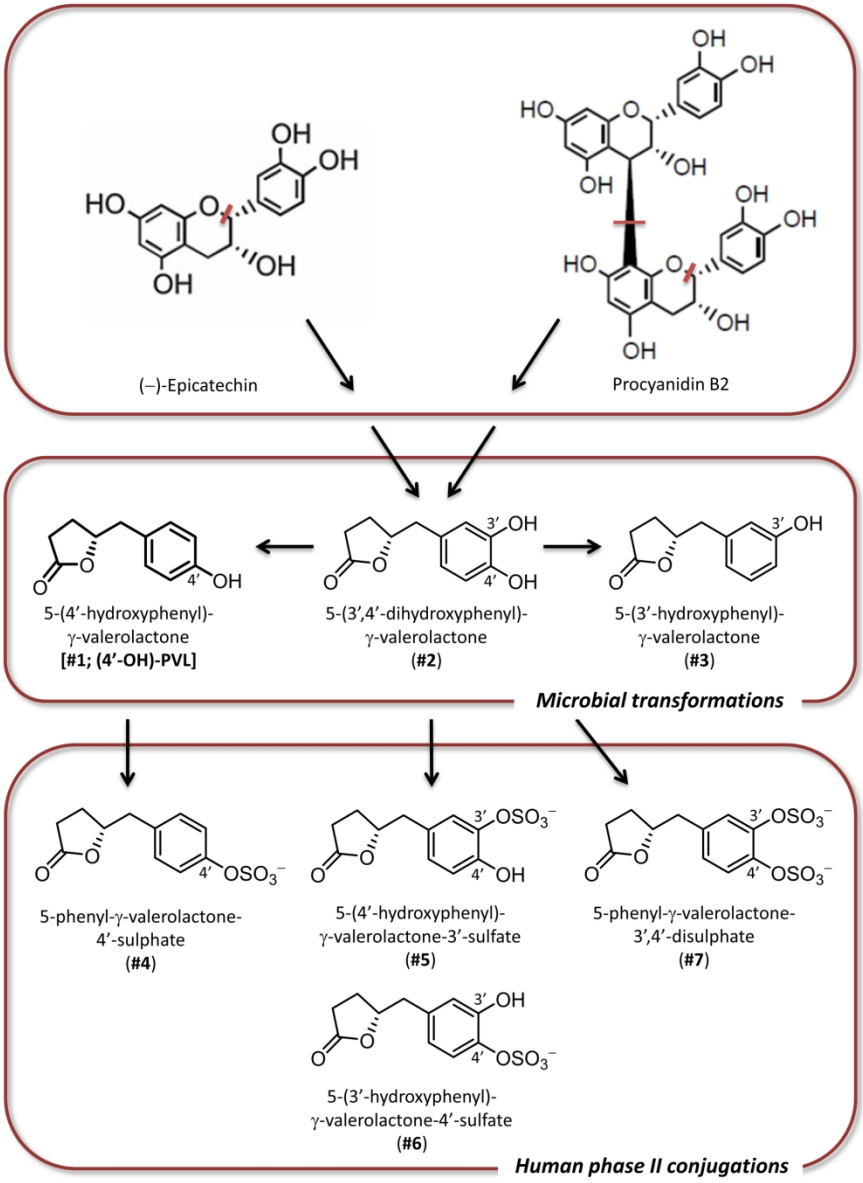

Figure 1. Outline of human flavan-3-ol metabolism and PVL formation. Starting from (–)-epicatechin and procyanidin B2, chosen as representative plant polyphenol precursors, after 5-carbon side-chain ring fission and initial transformation catalyzed by gut microbial enzymes, compounds #1-2 serve as precursors for subsequent phase II metabolism as indicated. The latter is catalyzed by host colonic and hepatic enzymes and generates the indicated sulfated PVL derivatives (compounds #4-7) as major products (collectively designated as 'phase II metabolites') that are then released into the circulation.

170x232mm (300 x 300 DPI)

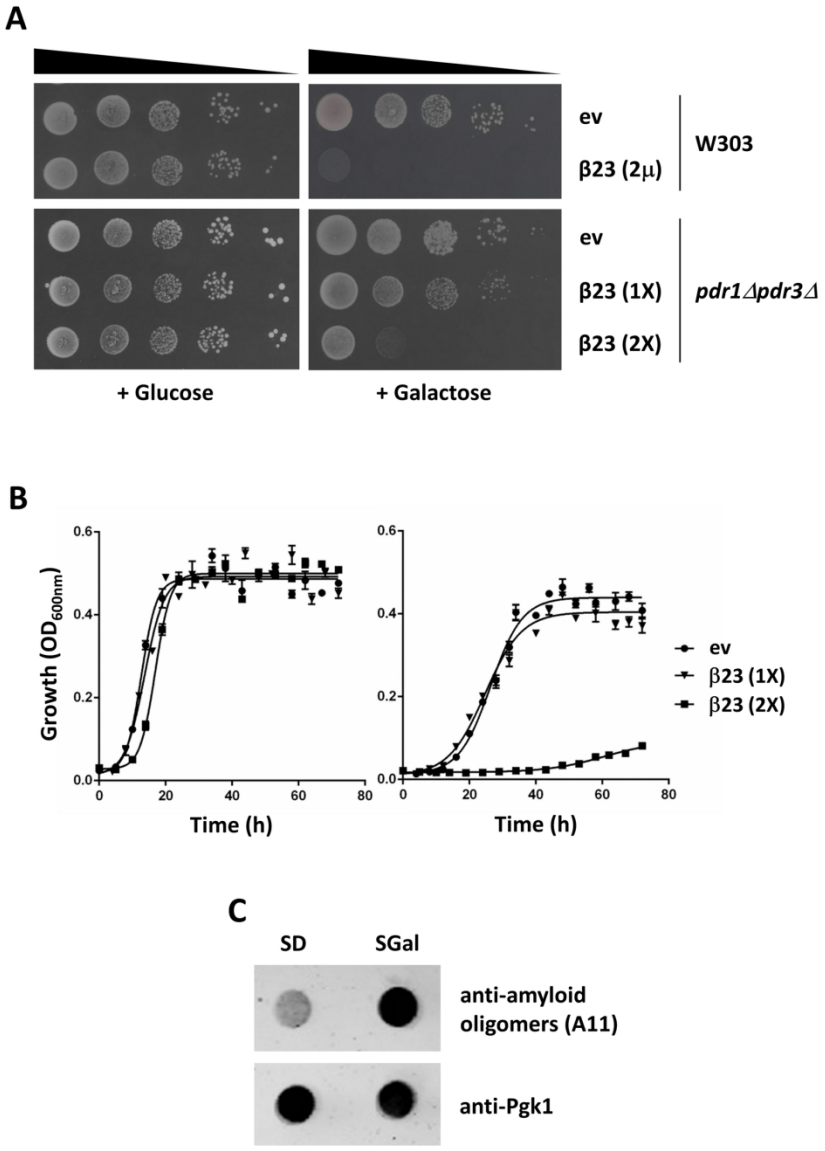

Figure 2. β23 amyloid oligomer formation and toxicity in yeast. A) Serial dilution assays (10-fold input cell dilutions ranging from 10^1 to 10^4) were performed on yeast cells transformed with either episomal (2μ) or integrative β23 [one-copy (1X); two-copy (2X)] constructs; empty-vector (ev) transformants served as controls. Cells were spotted on glucose- or galactose-containing agar plates and growth was assessed after 2 days at 30°C. B) Growth curves of the 1X and the 2X β23 integrative transformants cultured under β23 expression repressive (+ glucose; *left*) or inducing (+ galactose; *right*) conditions. C) Immuno-dot blot analysis performed with the anti-amyloid oligomer antibody A11 on whole cell extract samples derived from the 2X β23 integrative transformant strain cultured in SD (glucose-containing) or SGal (galactose-containing) liquid medium. Immunoreactivity with the constitutively expressed phoshoglycerate kinase (Pgk1) enzyme served as a loading control.

149x202mm (300 x 300 DPI)

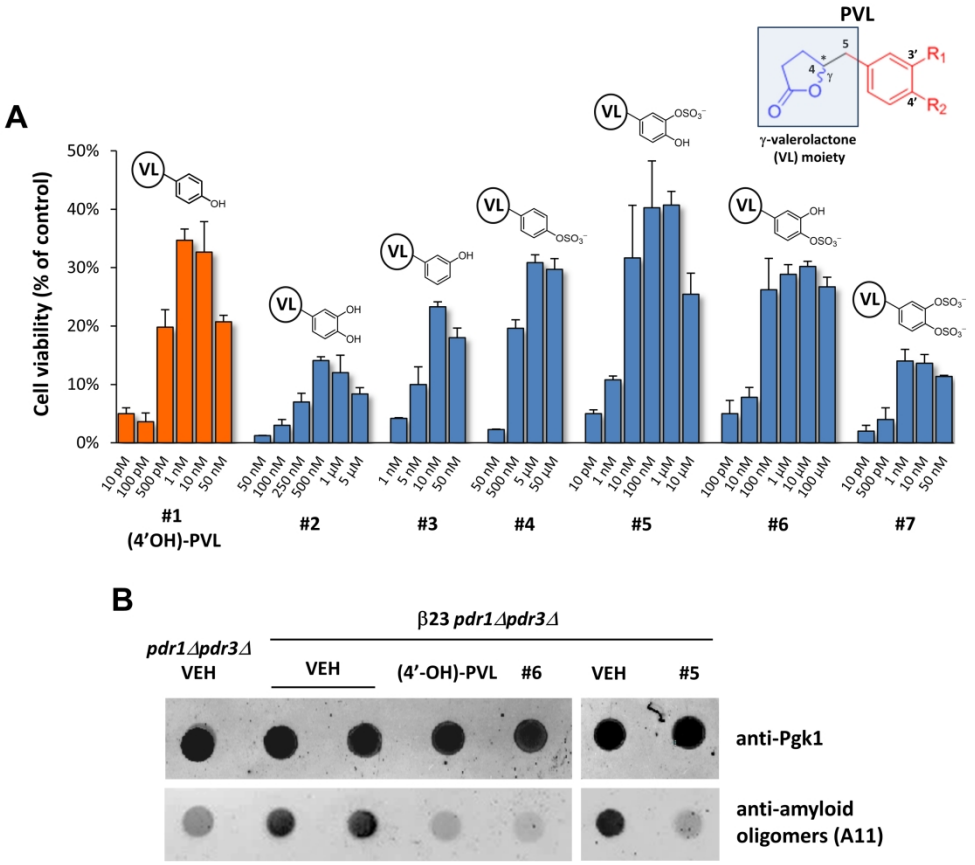

Figure 3. PVLs protect against β23 toxicity and reduce the accumulation of A11-reactive amyloid oligomers in yeast cells. A) Dose-response plots of the protective effects of the different PVLs. The results are expressed as percentage of 2X β23 cell viability relative to the vehicle (VEH; arbitrarily set to 0%); data are the mean ± SD of three replicates. A schematic representation of the chemical structures of the tested PVLs is shown above individual bar-plots. B) Immuno-dot blot analysis performed with the A11 antibody on total lysates from 2X β23 cells cultured under inducing (+ galactose) conditions in the presence of the indicated PVLs or the vehicle. *Pdr1Δpdr3Δ* cells treated with the vehicle served as reference; Pgk1 immunoreactivity was used as a loading control.

169x153mm (600 x 600 DPI)

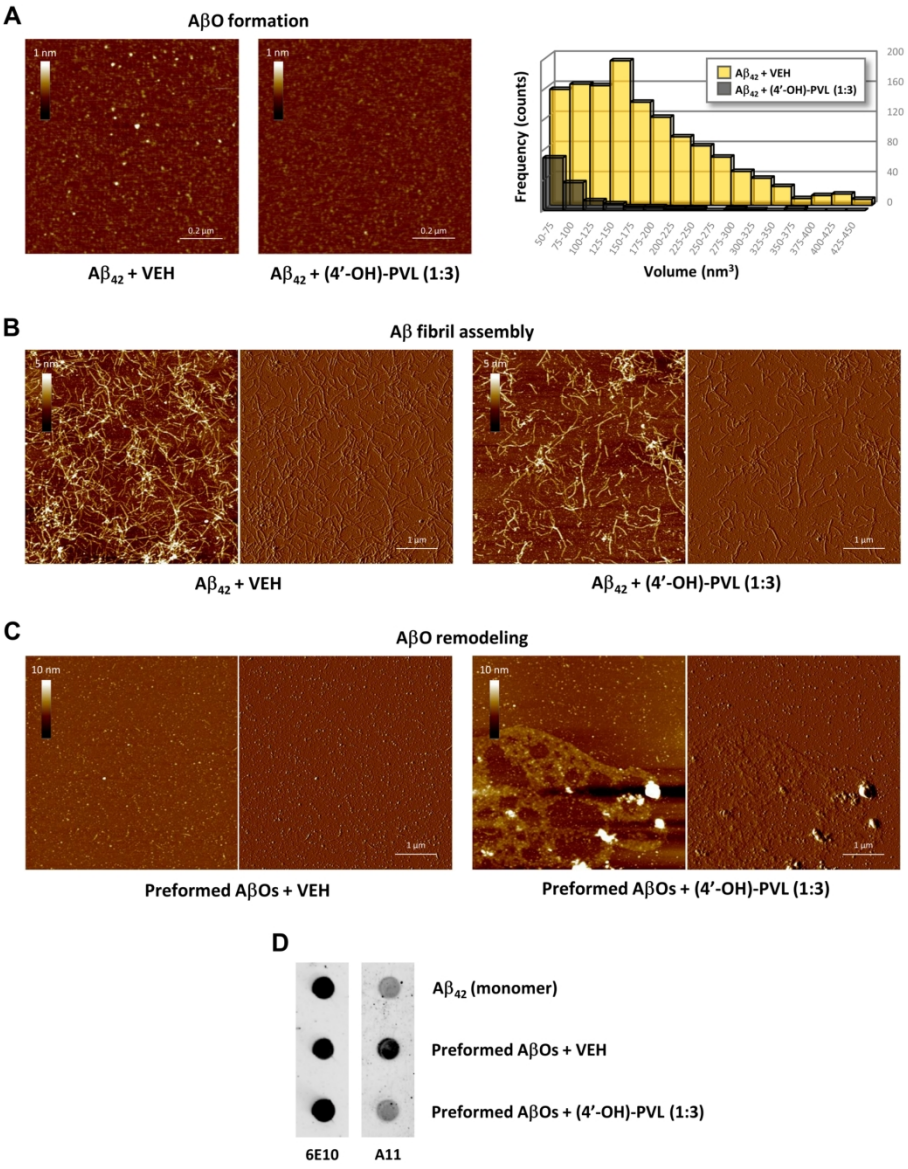

Figure 4. (4'-OH)-PVL interferes with Aβ$_{42}$ oligomer but not fibril formation and remodels preformed AβOs. A) AβOs were produced by incubating the synthetic human Aβ$_{42}$ depsipeptide for 24 h at 4°C (pH 7.4) in the presence of (4'-OH)-PVL (1:3 Aβ$_{42}$:PVL molar ratio), or the vehicle (VEH). A histogram quantification of the number ('frequency') and size ('volume') of the AβOs formed in the presence or absence of (4'-OH)-PVL is shown in the right-side panel. B) Same experimental set-up as in (A), but with a 4-days incubation at 37°C (pH 5.0) to allow for fibril formation. For each sample, height and amplitude AFM images are shown. C) Preformed AβOs produced as in (A) were diluted 10-fold with PBS supplemented with either (4'-OH)-PVL (1:3 monomeric Aβ$_{42}$:PVL molar ratio) or vehicle and incubated at 22°C for 3 h prior to AFM analysis. D) Immuno-dot blot analysis of preformed AβOs treated with (4'-OH)-PVL or the vehicle as in (C). The Aβ sequence-specific (6E10) and the oligomer conformation-specific (A11) antibodies were used as loading control and test antibodies, respectively. The monomeric (freshly dissolved) Aβ$_{42}$ peptide served as a negative control for A11-immunoreactivity.

169x215mm (300 x 300 DPI)

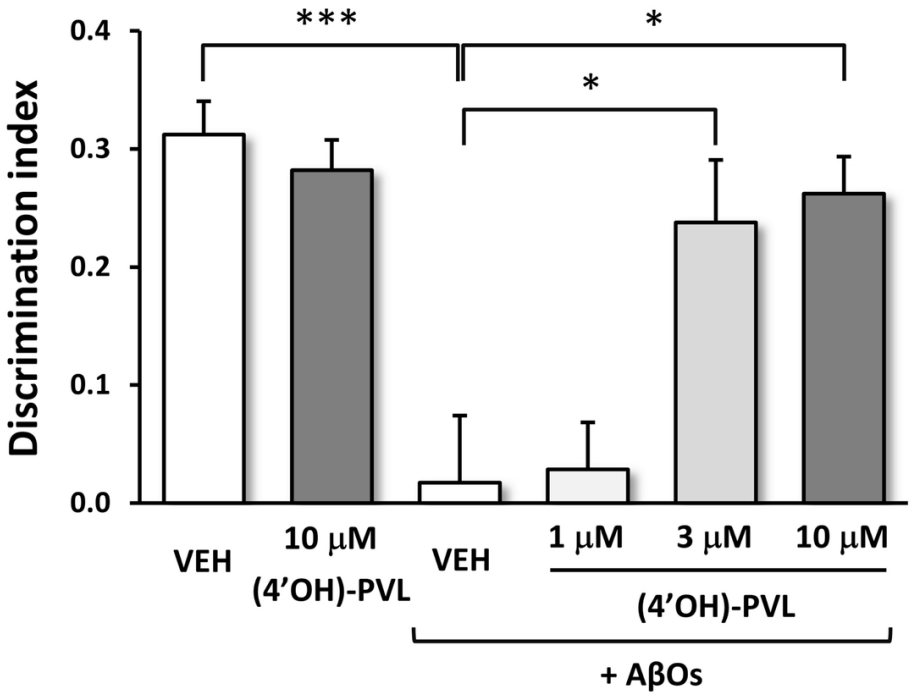

Figure 5. (4'-OH)-PVL antagonizes AβO-mediated memory impairment. Histogram representation (mean ± SEM) of the Discrimination Index (see 'Experimental Section') measured by NORT in mice ICV-injected with AβOs (1 μM monomeric $A\beta_{42}$) preincubated with the vehicle (VEH; n=18) or the indicated concentrations of (4'-OH)-PVL [1 μM (n=7); 3 μM (n=21); 10 μM (n=10)]. Two additional groups of animals, ICV-injected in parallel with the vehicle (n=21) or with the highest concentration of (4'-OH)-PVL (10 μM; n=8) without AβOs served as controls. The significant memory deficit observed in the AβOs+VEH group compared to the VEH only group was dose-dependently antagonized by (4'-OH)-PVL (* $p<0.05$, *** $p<0.001$; Tukey's test).

99x77mm (300 x 300 DPI)

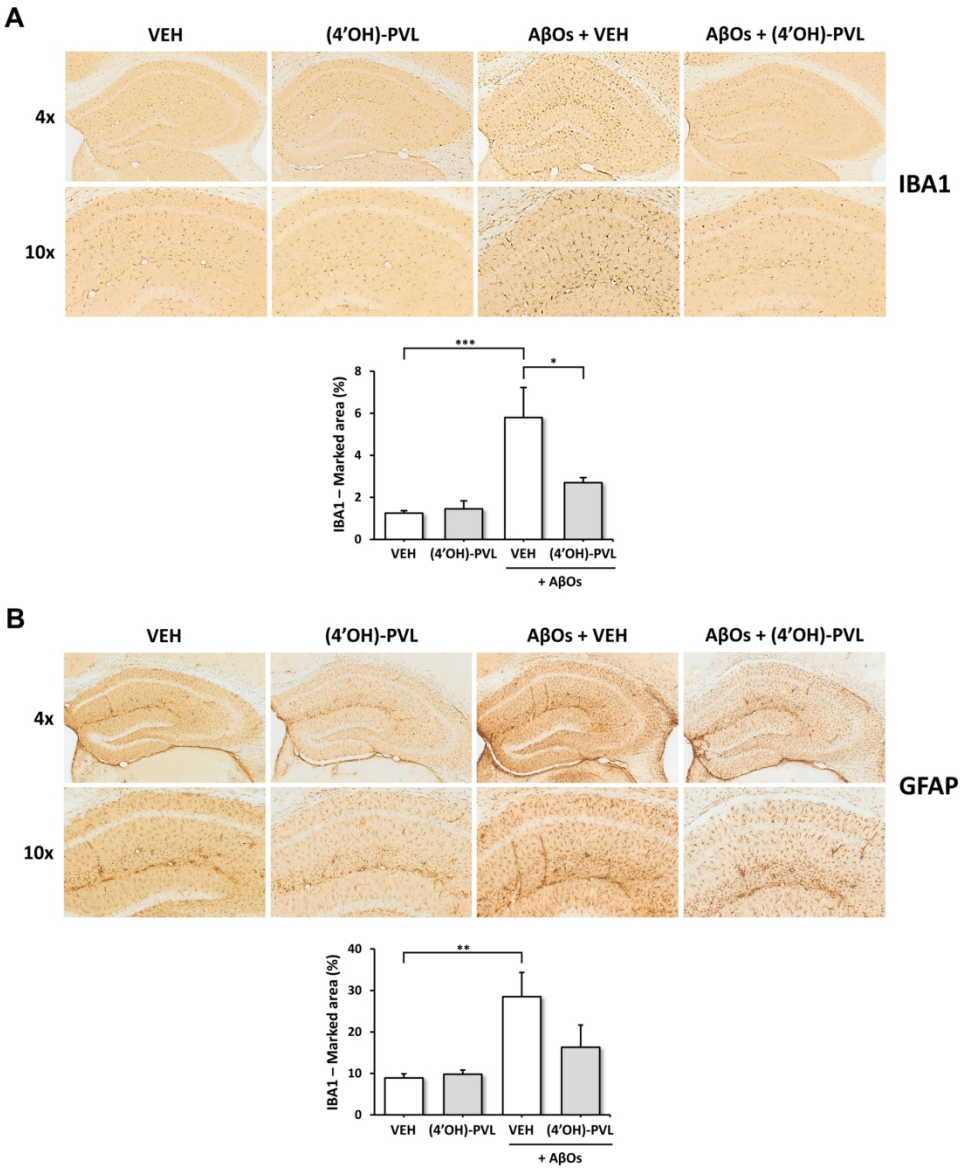

Figure 6. (4'-OH)-PVL treatment reduces glial activation in AβO-treated mice. A) Hippocampal slices from mice microinjected with the vehicle (VEH, n=8), (4'-OH)-PVL (3 μM; n=8), preformed AβOs (1 μM monomeric $A\beta_{42}$) preincubated with VEH (n= 9), or with (4'-OH)-PVL (3 μM; n=9), were immuno-stained with an antibody against the microglia/macrophage-specific protein Iba1. Immunoreactivity data (mean ± SEM) are reported in the histogram shown below the immuno-microscopy images (* $p<0.05$, *** $p<0.001$; Tukey's test). B) Same as (A) except for the use of an antibody directed against the glia/astrocyte intermediate filament protein GFAP for immunostaining (** $p<0.01$).

172x207mm (300 x 300 DPI)

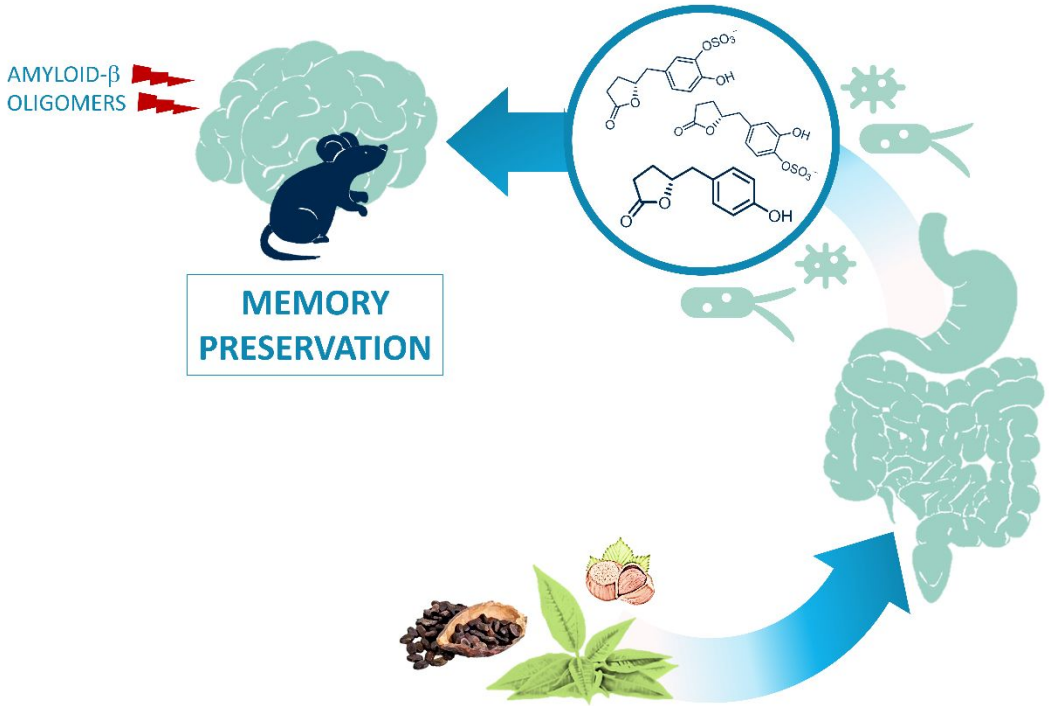

Circulating phenyl-valerolactone-based metabolites, derived from cocoa and other flavan-3-ol-rich foods through combined, microbial and human cell-mediated bioconversion, selectively detoxify amyloid-β oligomers, the most proximal causative agents of Alzheimer's disease.